JOURNAL OF MATERIALS SCIENCE 21 (1986) 1889–1896

Rapidly solidifed Al–Cr alloys: structure and decomposition behaviour

L. BENDERSKY
Center for Materials Research, The Johns Hopkins University, Baltimore, Maryland 21218, USA
R. J. SCHAEFER, F. S. BIANCANIELLO
Metallurgy Division, Center for Materials Science, National Bureau of Standards, Gaithersburg, Maryland 21771, USA
D. SHECHTMAN
Department of Materials Engineering, Technion, Haifa, Israel

Melt-spun ribbons of aluminium containing up to 15 wt% chromium were examined in the as-spun condition and after annealing. The more concentrated alloys contained multi-phase spherulites embedded in an α-Al matrix: chemical microanalysis showed the average composition of the spherulite core to be 22 ± 2 wt% chromium. The kinetics of precipitation at grain boundaries and within the matrix were determined by TEM and X-ray diffraction. Three very similar Al–Cr intermetallic phases are present under equilibrium conditions, but most of the precipitates in the melt-spun ribbons could be identified as Al_7Cr.

1. Introduction

Transition metals are commonly used as alloying elements to aluminium. Although they do not produce age hardening, they are added for various purposes, such as mechanical property improvement, recrystallization inhibition, stress corrosion prevention, etc. Due to the unfavourable electrochemical factor and the tendency of the components to form intermetallic phases, the range of solid solubility is extremely limited. It can, however, be significantly extended by rapid solidification [1–3]. The substantial increase in solid solubility offers the prospect of developing new alloy compositions with improved thermal stability. Several such additives as chromium, manganese and zirconium offer resistance to solute clustering during (or following) quenching [4, 5].

Rapidly solidified Al–Cr alloys exhibit a pronounced tendency to form metastable supersaturated solid solutions. This system has been investigated by several authors [5–15] who used different techniques of rapid quenching from the melt. Most previous studies [10–12, 14, 15] were limited to compositions of up to 3 wt% Cr, and some of them lack microstructural studies. Detailed electron microscopy investigation was performed by Warlimont *et al.* [8, 9] and Jones *et al.* [2, 5, 6]. Their studies were performed on compositions of up to 13 wt% Cr, and included study of the decomposition behaviour. These works are the main references for us.

In the present study we examined the microstructure of melt-spun ribbons which contain up to 15 wt% Cr. Thermal stability and decompositional behaviour were studied as a function of the chromium content and the temperature of isochronal heat treatment.

2. Experimental details

Alloy buttons with chromium concentrations of 1, 2, 5 and 15 wt% Cr were prepared by arc melting, using 99.999% Al and 99.95% Cr. For melt-spinning, small pieces cut from these buttons were induction heated in zirconia-coated quartz tubes. Immediately upon melting, the metal was squirted onto a copper melt-spinning wheel rotated at 6500 r.p.m. The process was carried out under helium at atmospheric pressure. The ribbons were typically 2 mm wide and 20 μm thick. For annealing, the ribbons were sealed in borosilicate glass ampoules with a helium pressure of 1/2 atmosphere.

Lattice parameters were determined by measurements on an X-ray diffractometer, using filtered CuK_α radiation. A Nelson–Riley procedure was used to obtain the lattice parameter from the measurements of the diffraction peaks. Simultaneous measurements of diffraction peaks from powdered high purity silicon were used as a normalization standard.

Three phases of apparently very similar crystal structure have been reported in aluminium rich Al–Cr alloys [16]: Al_7Cr or θ (21.6 wt% Cr), $Al_{11}Cr_2$ or η (25.96 wt% Cr) and Al_4Cr or ε (32.52 wt% Cr) are reported [9] to be very similar and no information on differences between them has been reported. We therefore prepared samples having the stoichiometric compositions of these compounds as X-ray diffraction references. These samples were first melt spun to reduce microsegregation, crushed and sieved to −325 mesh, and annealed at 600° C for 16 h. X-ray diffraction patterns from these powders, using CuK_α radiation, were then compared.

Microstructural studies were performed on a

0022–2461/86 $03.00 + .12

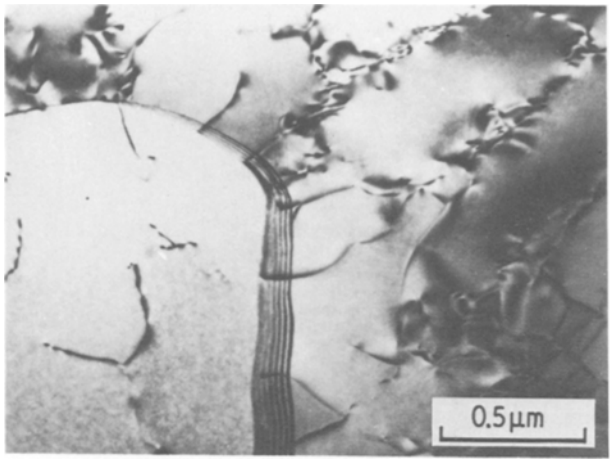

Figure 1 As-spun ribbon of Al–2 wt % Cr alloy. A dislocation substructure is probably associated with slight microsegregation.

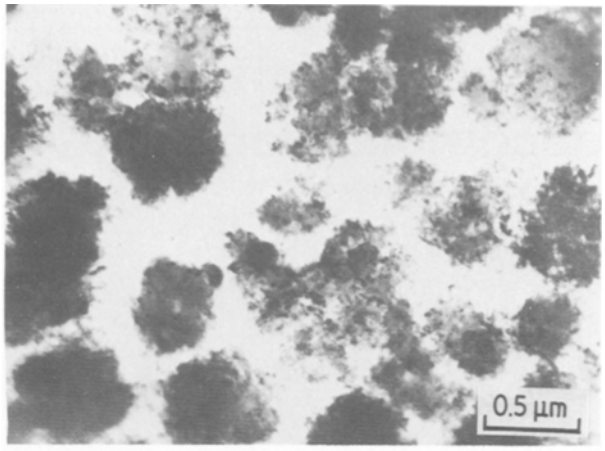

Figure 2 As-spun ribbon of Al–15 wt % Cr alloy. Spherulites embedded in aluminium matrix.

scanning transmission electron microscope. Chemical microanalysis was performed in the scanning transmission mode using a 5 nm probe. Quantification of the X-ray information was accomplished by using the Cliff–Lorimer method [17, 18], when the condition of the thin film approximation was maintained. X-ray intensity relates to composition by the expression $C_A/C_B = k_{AB}I_A/I_B$, where I_A and I_B are the measured characteristic X-ray intensities, and C_A and C_B are the weight fractions of two elements A and B (in our case aluminium and chromium). The coefficient $k_{Cr/Al}$ (constant in the thin film approximation) was found experimentally using the known phase θ-Al_7Cr as a standard: $k_{Al/Cr} = 0.91 \pm 0.1$.

The ribbons were thinned for STEM study by jet electropolishing in a standard solution.

3. Results

3.1. As-spun ribbons (TEM analysis)

The 1 and 2 wt % Cr alloys are one-phase supersaturated solid solutions of chromium in aluminium (maximum equilibrium solubility is 0.77 wt % Cr [18]). No second phase can be observed. A dislocation substructure is present and is probably associated with slight cellular microsegregation (see Fig. 1).

The 5 wt % Cr alloy has a transition microstructure between low and high concentration of chromium. In some regions the microstructure consists of one-phase grains of supersaturated (5 wt % chromium) α-Al, with slight evidence of cellular structure and dislocation substructure (like the 1 and 2 wt % Cr alloys). In other regions the microstructure is characterized by multi-phase spherulites, embedded in α-Al matrix. Their volume fraction increases with increase of chromium concentration to reach homogeneous high density in the 15 wt % Cr alloy (see Fig. 2). The formation of spherulites was reported for the Al–Cr system by Furrer and Warlimant [9] and for several other systems by Shechtman and Horowitz [19].

The spherulites are generally composed of a core A (see Fig. 3a), surrounded by small petal-like crystals B measuring ~ 50 nm in size. The contrast of the petals is sometimes enhanced by Moiré fringes. The core has a two-phase structure, composed of very fine particles of size smaller than 5 nm. In some cases the spherulites are without petals on the periphery, as was found by Furrer and Warlimont [9]. Chemical microanalysis shows that the average composition of the core is 22 ± 2 wt % Cr. The composition of the matrix surrounding the spherulites is ~ 5 wt % Cr. A typical concentration profile of the microstructure is shown in Fig. 4, where gradual transition from 22 to 5 wt % Cr reflects a decrease in the density of petals embedded in the α-Al matrix. Dark field micrographs obtained with

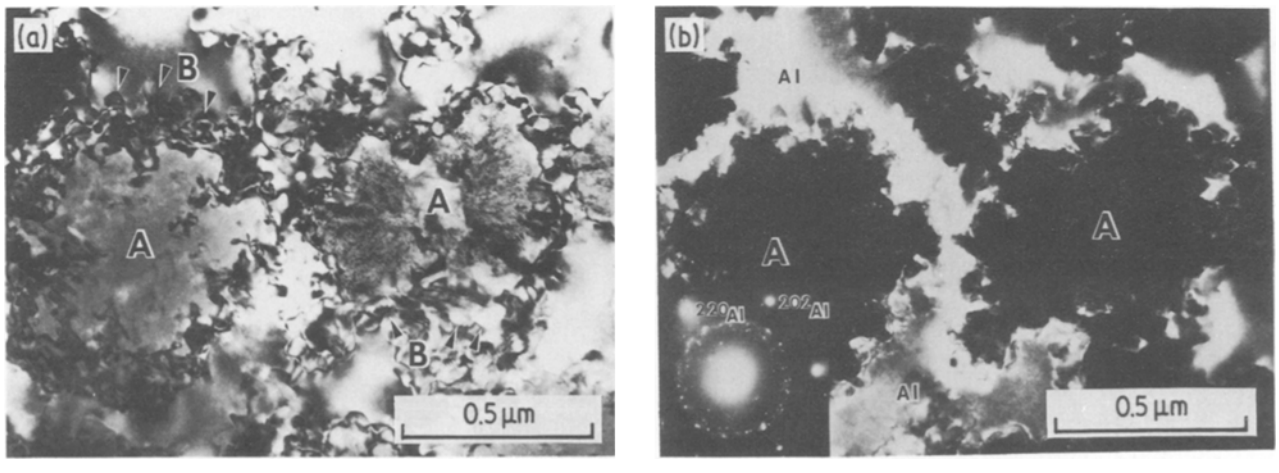

Figure 3 As-spun ribbon of Al–15 wt % Cr. (a) Bright field image of spherulites. The spherulites are composed of a core A, surrounded by petal-like crystals B (marked by arrow); (b) Dark field using an Al-matrix reflection. Surrounding matrix is α-Al.

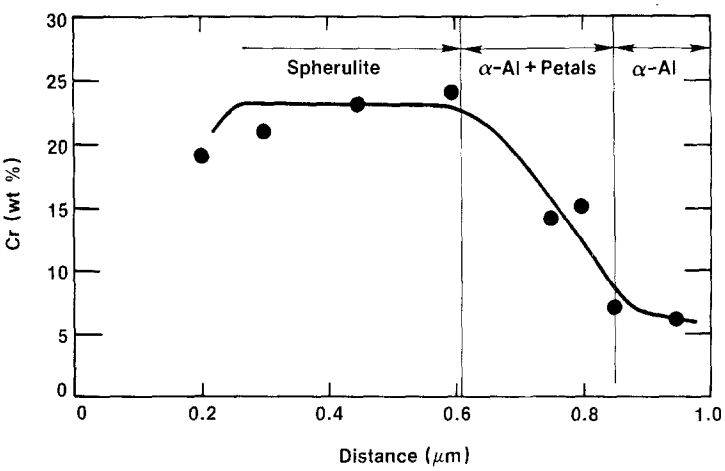

Figure 4 Composition profile across a spherulite.

an aluminium reflection (see Fig. 3b) confirms that the surrounding matrix is α-Al. A series of convergent beam diffraction patterns taken from different spherulites in the same matrix show that the spherulites are randomly oriented. These diffraction patterns are a combination of two or more single patterns of intermetallics with orientational coherence between them. No aluminium reflections were found here. This contradicts some results obtained by Furrer and Warlimont [9] who concluded that spherulites are composed of randomly oriented precipitates within the aluminium matrix.

Analysis of convergent beam diffraction patterns from the petals shows that they have the structure of the θ-Al_7Cr phase (see Fig. 5), which is monoclinic with $a = 2.531\,nm$; $b = 0.754\,nm$; $c = 1.0949\,nm$; $\beta = 128°\ 71'$ [20]. Dark field micrographs (Fig. 6) obtained with an intermetallic reflection show the possibility that the petals and at least one group of fine precipitates in the core have the same structure.

3.2. Heat treated ribbons (TEM analysis)

The decomposition behaviour of the alloys was studied in the range of temperatures 250 to 550° C for composition of 1, 2 and 5 wt % Cr. For most cases the annealing time was 6 h, however for some up to 100 h. Generally, supersaturated aluminium decomposes at the grain boundaries and within grains to form needle- or plate-like precipitates of the equilibrium phase θ-Al_7Cr, with no indication of any transition phase, in agreement with others [5, 6, 15].

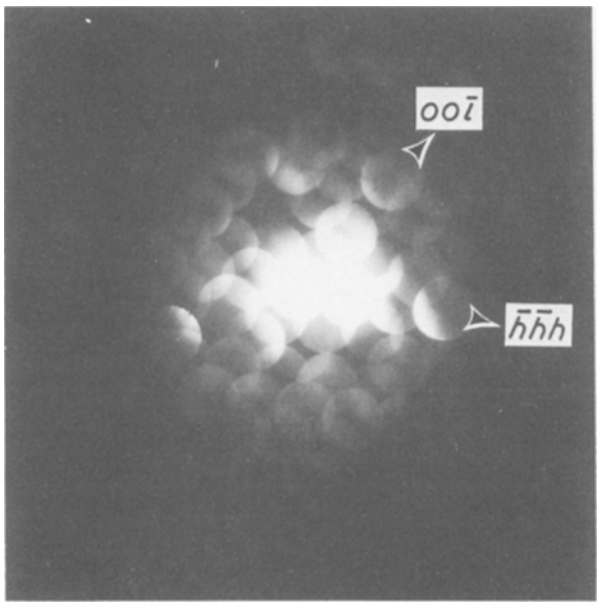

Figure 5 Microdiffraction from the "petal" [1 1 0] zone axis of Al_7Cr. Arrows show directions (0 0 l) and ($h\,h\,h$) of reflection rows.

Analysis of samples annealed for 6 h shows that grain boundary precipitation (GBP) starts at a lower temperature than matrix precipitation (MP). The difference is roughly 50° C. The temperature at which decomposition starts (where the second phase is first observed) depends strongly on the degree of supersaturation. Fig. 7 shows the summarized results, where the curves represent the beginning of the GBP and MP decomposition. Annealing up to 100 h at temperatures of GBP start results in the appearance of only GB precipitates, without any matrix precipitation (see Fig. 8). At temperatures above the MP start curve, fast growth of matrix precipitates occurs, until the supersaturated matrix is completely relaxed (see Fig. 9). Selected area electron diffraction indicates that both grain boundary and matrix precipitates are θ-Al_7Cr (Fig. 10). It was found the longest axis of the precipitates is parallel to the $\langle 0\,1\,1\rangle_{Al}$ direction.

The microstructure after annealing at temperatures below the curve of GBP start (Fig. 7) is characterized by finely dispersed strain contrast (see Fig. 11). No distortion of diffraction spots or super-lattice reflections were found. Annealing at higher temperatures or for longer time does not change the character of diffraction, but the contrast appears to be more intensive (Fig. 12) and the centres of strain contrast are less dense. In certain cases it is possible to resolve it as loops (Fig. 13). These loops or clusters have very high thermal stability and exist up to 500° C (see Fig. 14).

3.3. X-ray studies

The measured lattice parameters of the as-spun 1, 2 and 5 wt % Cr ribbons are within 10^{-4} nm of the values collected by Midson *et al.* [5] for rapidly solidified alloys (Fig. 15). No indication of phases other than aluminium is seen in the X-ray diffraction patterns of these alloys. Upon annealing for 6 h, no significant change of lattice parameter is seen at temperatures of 400° C or less. At 450° C the lattice parameter of the 5 wt % Cr alloy has started to shift, and at 500° C the supersaturation of the 5% and 2% alloys has mostly disappeared (Fig. 15).

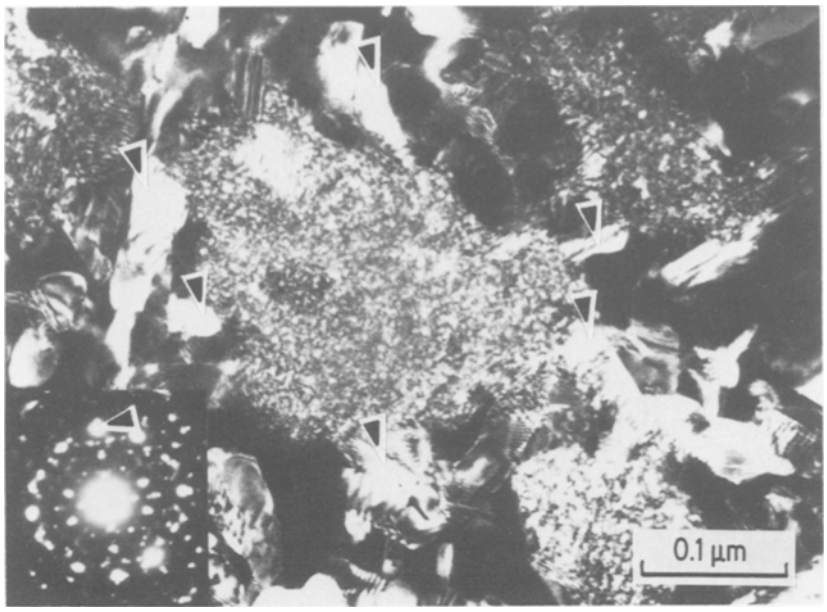

Figure 6 Dark field using an intermetallic reflection. Fine precipitates in spherulite core and some petals (marked by arrows) reflect at the same time.

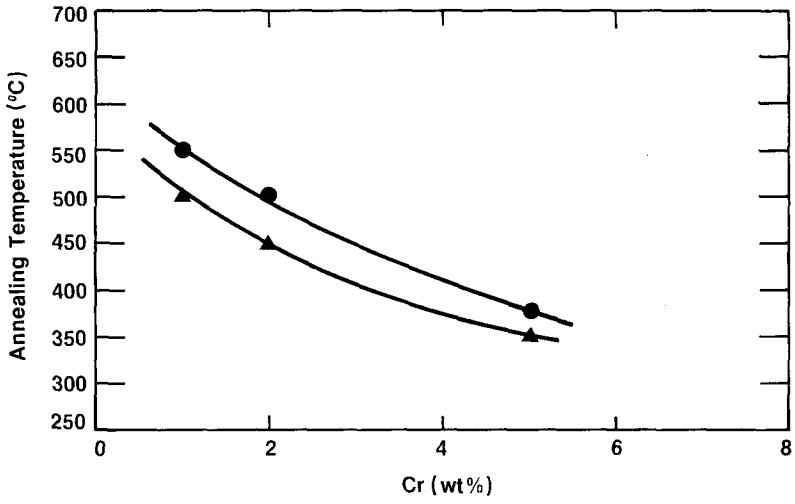

Figure 7 Annealing temperature–composition diagram, where curves represent the beginning of precipitation (▲) on grain boundaries (GBP) and (●) inside the grains (MP) for 6 h anneals.

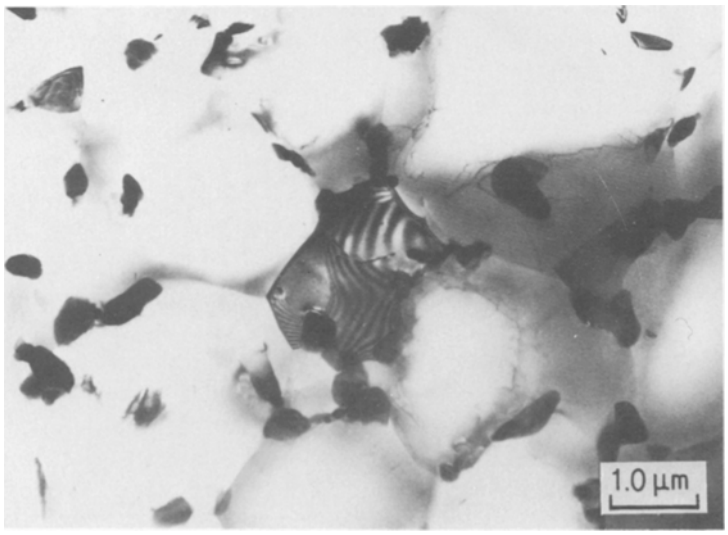

Figure 8 The Al–2 wt % Cr following 100 h at 400° C containing Al_7Cr particles mostly along grain boundaries.

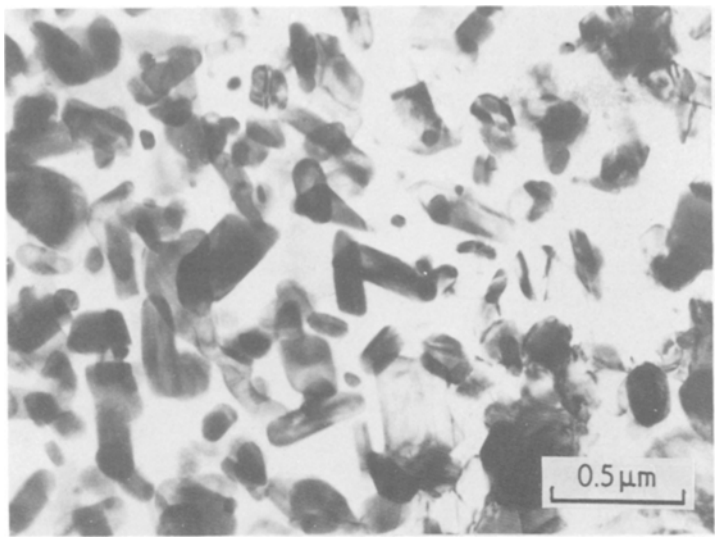

Figure 9 The Al–5 wt % Cr following 6 h at 550° C containing Al_7Cr particles within the grains.

X-ray diffraction peaks from intermetallic phases are first seen after 6 h at temperatures as low as 400° C (Fig. 16) and become progressively stronger at higher temperatures. Analysis of alloys having stoichiometric compositions shows that only the θ-Al_7Cr sample had a peak at $2\theta = 21.7°$, only the ε-Al_4Cr sample had peaks at $2\theta = 17°$ and 26.6°, and the η-$Al_{11}Cr_2$ sample showed none of these peaks. In addition, there was a substantial difference in the detailed distribution of intense peaks in the region between $2\theta = 36$–46°, with the pattern from the θ-Al_7Cr sample corresponding well to a pattern computed from structural data reported for this phase [20] as shown in Fig. 16. It should be noted that the diffraction patterns of these samples were significantly different in the as-solidified condition and after annealing at 600° C, as would be expected from the phase diagram.

On the basis of the diffraction patterns of the reference samples, the precipitates in the annealed ribbons are identified as shown in Fig. 17. In the earlier stages of precipitation, however, the phase identification can only be tentative.

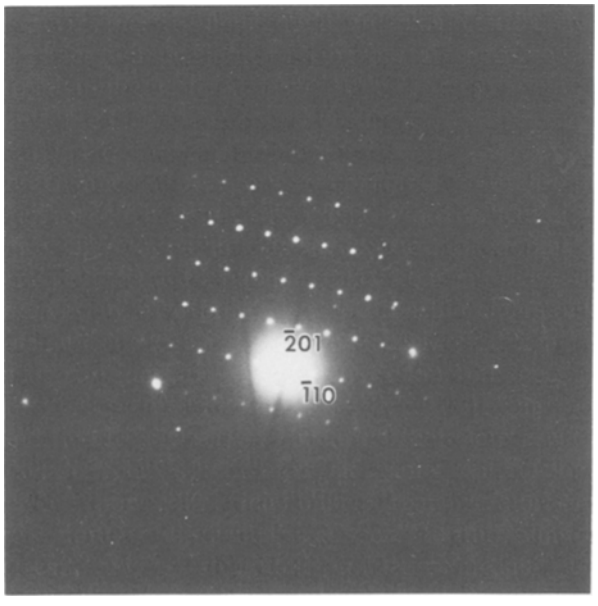

Figure 10 Diffraction pattern typical for both grain boundary and matrix precipitates. [1 1 2] axis zone of Al_7Cr.

The diffraction pattern of the as-spun 15 wt % Cr alloy shows peaks corresponding to the icosahedral phase [21] as well as peaks which could be attributed to any of the equilibrium phases θ, η or ε. After annealing for 6 h at 350° C or higher, intermetallic peaks clearly corresponding to θ-Al_7Cr are observed. An as-spun ribbon containing 20 wt % Cr showed diffraction peaks only from α-Al and the icosahedral phase, with none from θ, η or ε.

4. Discussion

Highly extended solid solubility can be achieved for melt-spun ribbons of Al–Cr. In our experiments the extension is up to 5 wt % Cr, and we believe that it is close to the maximum one can get by this technique of melt quenching. The maximum was established to be 7 wt % Cr for two-piston [5] and splat [9] quenching for a thickness of $\sim 50\,\mu$m. Higher values up to 10 wt % Cr were attainable for very thin sections, e.g. of gun splats [8, 9, 22]. These differences in solid solubility maximum reflect the sensitivity to the changes in cooling rate in the range 10^6 to 10^8 K sec^{-1} and to the degree of supercooling, accordingly [7].

Aluminum containing small concentrations of chromium is expected to solidify without microsegregation at relatively low velocities on the basis of the absolute stability effect of morphological stability theory [23]. Because the solute partition coefficient in this system is relatively close to unity (although not known with precision), the absolute stability effect is predicted to occur at relatively low velocities (or high concentrations) compared to a system such as Al–Fe [19], where the solute partition coefficient is extremely small. This effect accounts for the absence or rarity of cellular substructures in the alloys containing 1, 2 or 5 wt % Cr.

At higher concentration (> 5 wt % Cr) the competitive solidification of intermetallic phases begins. They appear within the liquid and grow as spherulites to $\sim 1\,\mu$m diameter before being engulfed by the solidifying supersaturated alumium front. The spherulite volume density increases with increasing chromium concentration. For the 15 wt % Cr alloy the solidification of spherulites is the dominant mode. The appearance of spherulites influences the mechanical

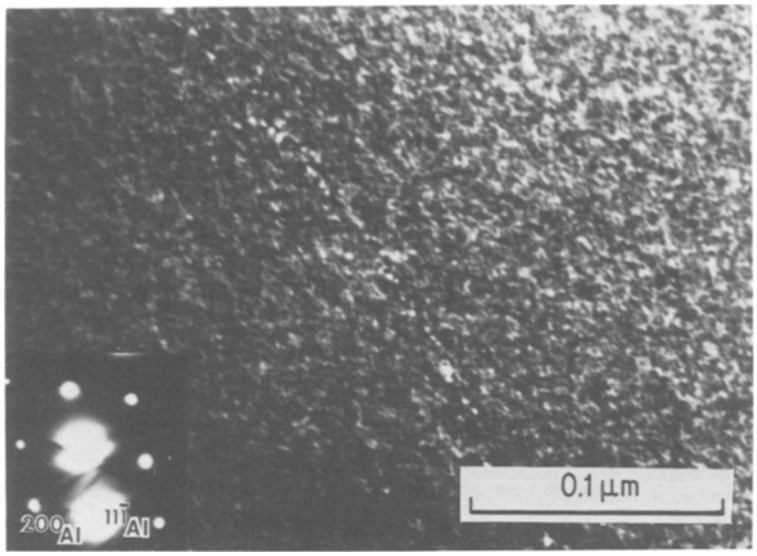

Figure 11 The Al–5 wt % Cr following 100 h at 300° C. Dark field using (1 1 1) reflection of aluminium. Fringe strain constrast. Diffraction pattern is entirely of α-Al.

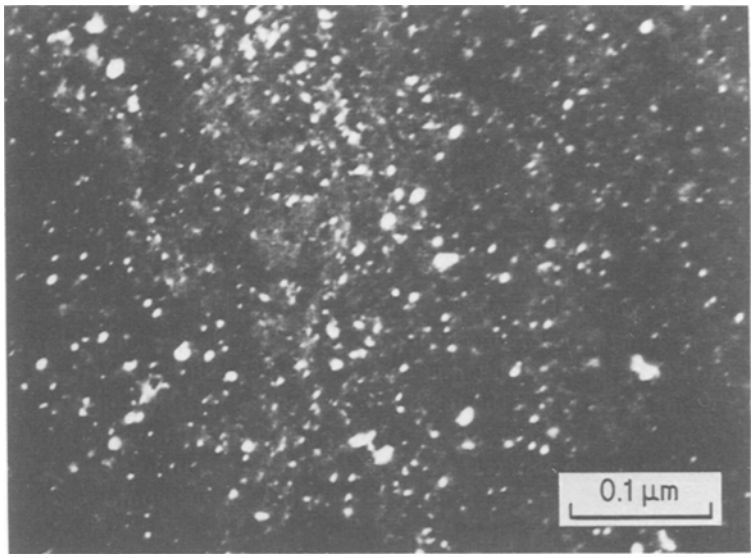

Figure 12 The Al–1 wt Cr following 6 h at 500° C. Dark field using (1 1 1) reflection of aluminium at weak beam condition. Strain contrast is enhanced compared to Fig. 13. Diffraction pattern is entirely of α-Al.

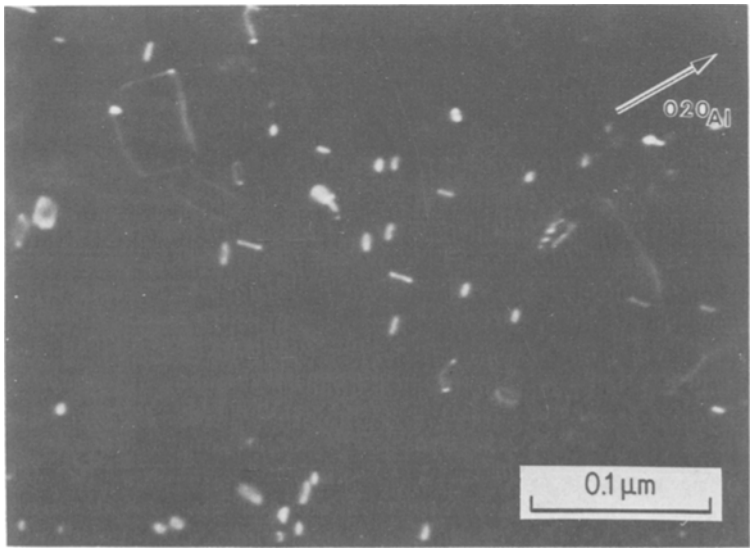

Figure 13 The Al–1 wt % Cr following 6 h at 450° C. Dark field using (0 2 0) reflection of aluminium at weak beam condition of dislocations loops.

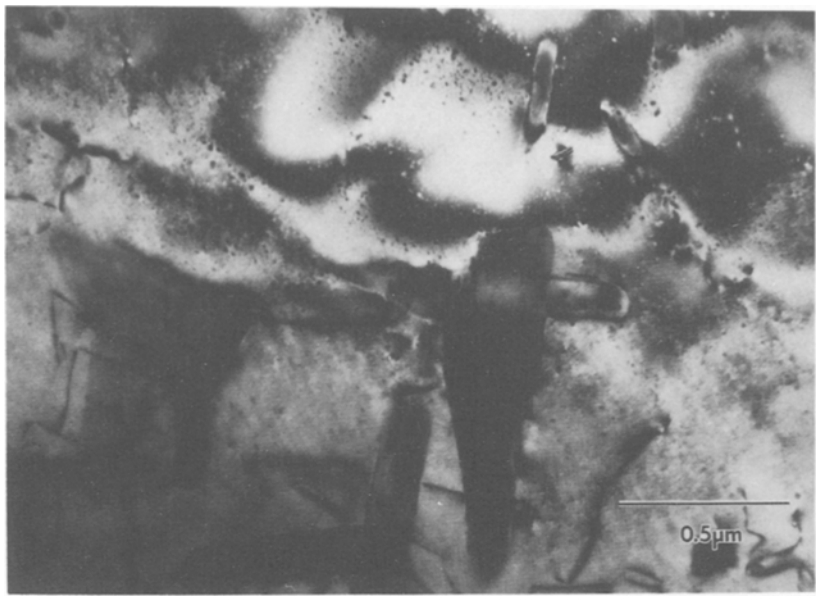

Figure 14 The Al–2 wt % Cr following 6 h at 500° C. Bright field micrograph shows coexistence of Al_7Cr precipitates and objects of strain contrast.

properties. For example, Yakunin *et al.* [24] reported decreasing tensile strength for alloys with compositions higher than 8 wt % Cr. Solidification as separated spherulites is an unusual pattern in rapid solidification, although common in concentrated aluminium–transition metal alloys, e.g. in Al–Fe (> 11 wt % Fe) and Al–Mn (> 15 wt % Mn) [19, 25]. The increase of spherulite volume density points out that the nucleation rate for the intermetallic phase starts to be dominant compared to the nucleation rate for α-Al as the concentration of the alloy increases. The steep increase of the intermetallic liquidus with concentration, compared to the slow change for the α-Al liquidus, provides different rates of change in supercooling with concentration. The supercooling as a function of chromium content changes very little for α-Al, while it strongly increases for the intermetallic. Accordingly, the relative nucleation rate depends on the concentration.

Equilibrium freezing concepts would predict that in the 5 wt % Cr alloy the η-$Al_{11}Cr_2$ phase would form first from the liquid and the θ-Al_7Cr phase would then form by a peritectic reaction, whereas in the 15 wt % Cr alloy, primary ε-Al_4Mn phase would form, followed by peritectic η and θ. Under rapid solidification conditions, however, the equilibrium phases may be suppressed. The core of the spherulites formed in the 15 wt % Cr alloy, which has a composition midway between that of the θ and η phases, could thus have initially solidified from the melt as any of the intermetallic phases and subsequently decomposed in the solid state during cooling of the ribbon into a mixture of θ and η.

It should be noted that the equilibrium boundaries of the θ, η and ε phases are not well established, and the θ and η phases are reported to be structurally identical [26]. The exact identification of the many very fine crystallites which appear in the rapidly solidified materials is therefore difficult, and even the prediction of the relative stability of the different phases is questionable.

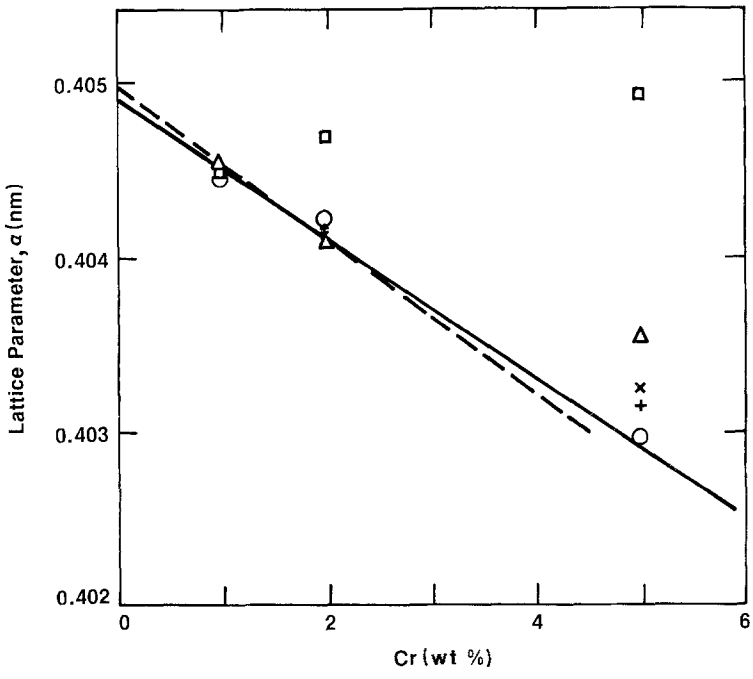

Figure 15 Lattice parameter of Al–Cr alloys, compared to data previously reported in (———) [3] and (– – –) [12]. (S+) as-spun. 6 h anneals at the following temperatures (○) 350° C, (×) 400° C, (△) 450° C, (□) 500° C.

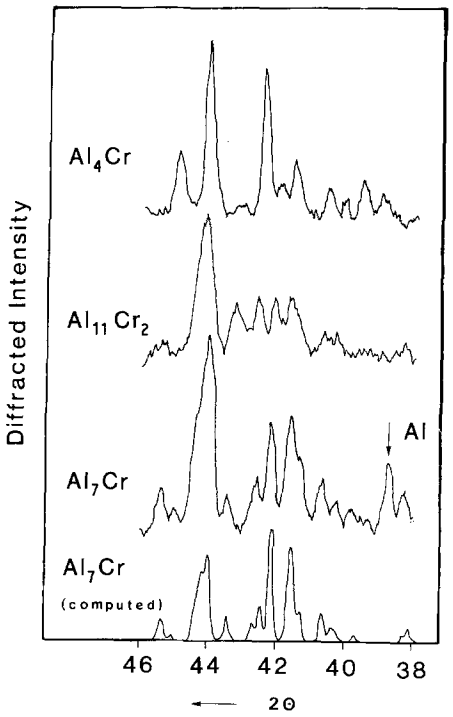

Figure 16 Diffraction patterns of CuK_α radiation from samples having the stoichiometric compositons of the Al–Cr intermetallic compounds. Samplers were melt spun, crushed, and annealed at 600° C for 16 h.

5. Conclusions

1. By melt-spinning, the concentration of chromium in solid solution in aluminium can be extended to approximately 5 wt %. As the chromium concentration is increased beyond 5 wt %, increasing numbers of chromium-rich spherulites are formed during solidification.

2. The spherulites have a core, consisting of very fine grains of two or more intermetallic phases, surrounded by petal-like crystals of the θ-Al_7Cr phase. The average composition of the core is 22 ± 2 wt % Cr.

3. Precipitation at grain boundaries occurs at temperatures lower than those which produce precipitation in the matrix. These temperatures are strongly dependent upon the sample composition.

Acknowledgement

The authors thank DARPA for financial support of this work.

References

1. H. JONES, *Aluminium* **54** (1978) 274.
2. S. P. MIDSON and H. JONES, in Proceedings of 4th International Conference on Rapid Quenched Metals, Sendai, 1981 (Japan Institute of Metals) p. 1539.
3. G. FALKENHAGEN and W. HOFMANN, *Zh. Metall.* **43** (1952) 69.
4. H. JONES, "Vacancies 76" edited by R. E. Smallman and J. E. Morris (The Metals Society, London, 1977) p. 175.
5. S. P. MIDSON, R. A. BUCKLEY and H. JONES, Proceedings 4th Conference on Rapidly Quenched Metals, Sendai, 1981 (Japan Institute of Metals) p. 1521.
6. H. JONES, "Rapid Solidification Processing, Principles and Technology II," edited by R. Mehrabian, B. Kear and M. Cohen (Claitor's, Baton Rouge, 1980) p. 306.
7. R. ICHIKAWA, T. OHASHI and T. IKEDA, *Trans. Jpn. Inst. Metals* **12** (1971) 280.
8. H. WARLIMONT, W. ZINGG and P. FURRER, *Mater. Sci. Eng.* **23** (1976) 101.
9. P. FURRER and H. WARLIMONT, *ibid.* **28** (1977) 127.
10. N. I. VARICH and R. B. ZYUKEVICH, *Russian Metall.* **4** (1970) 58.
11. *Idem, Izv. Acad. Nauk. Met.* **4** (1970 82.
12. A. F. POLESYA and A. I. STEPINA, *Fiz. Met. Metall.* **27** (1969) 885.
13. R. D. VENGRENOVICH and V. I. PSAREV, *ibid.* **29** (1970) 540.
14. V. I. DOBATKIN, V. I. ELAGIN, V. M. FEDOROV and R. M. SIZOV, *Izv. Acad. Nauk, Metall*, **2** (1970) 199.
15. K. NAGAHAMA and I. MIKI, *Trans. Jpn. Inst. Metals* **15** (1974) 185.
16. A. J. BRADLEY and S. S. LU, *J. Inst. Metals* **60** (1937) 319.
17. G. CLIFF and G. W. LORIMER, *J. Microsc.* **62** (1975) 246.
18. N. J. ZALUZEC, "Introduction to Analytical Electron Microscopy," edited by J. J. Hren, J. I. Goldstein and D. C. Joy (Plenum, 1979) p. 121.
19. D. SHECHTMAN and E. HOROWITZ, "Metastable Phases of Rapidly Solidified Al-Rich Al-Fe Alloys," Quarterly Reported DARPA Order No. MDA-903-83-K-0400, January (1984).
20. M. J. COOPER, *Acta Cryst.* **13**(1960) 257.
21. D. SHECHTMAN, I. BLECH, D. GRATIAS and J. W. CAHN, *Phys. Rev. Lett.* **53** (1984 1951.
22. L. M. BUROV and A. A. YAKUNIN, *Russ. J. Phys. Chem.* **42** (1968) 540.
23. S. R. CORIELL, R. F. SEKERKA, *J. Crystal Growth* **61** (1983) 499.
24. A. A. YAKUNIN, L. F. SILKA and A. B. LISENKO, *Fiz. Met. Metall.* **56** (1983) 945.
25. D. SHECTMAN, private communication (1984).
26. R. P. ELLIOTT, "Constitution of Binary Alloys, First Supplement," (McGraw-Hill, New York, 1965) p. 33.

Received 5 November 1984
and accepted 11 July 1985

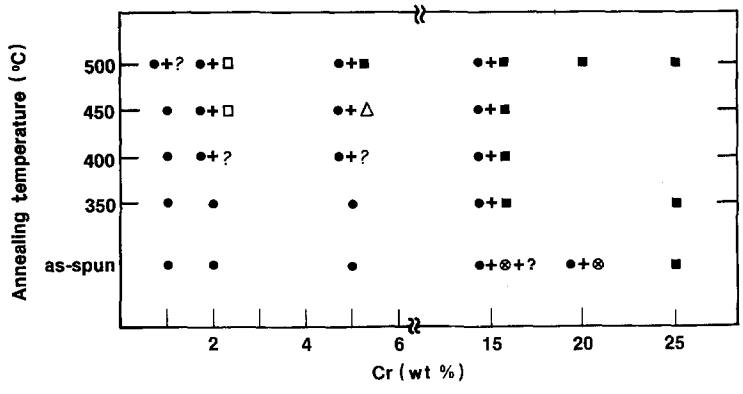

Figure 17 Phases observed by X-ray diffraction in melt-spun and annealed Al–Cr ribbons. 6 h anneals. (●) Aluminium, (■) Al_7Cr; (□) tentative, (▲) $Al_{11}Cr_2$; (△) tentative, (⊗) icosahedral phase, (?) indistinguishable, Al_7Cr, $Al_{11}Cr_2$, or Al_4Cr.